ICI Reduction Through Shaped OFDM in Coded MIMO-OFDM Systems

Wei Xiang, Julian Russell
Faculty of Engineering and Surveying
University of Southern Queensland
Toowoomba, QLD 4350
E-mail: xiangwei@usq.edu.au

Yafeng Wang
Wireless Theories & Technologies Laboratory
Beijing University of Posts and Telecommunications
Beijing 1000876, China
E-mail: wangyf@bupt.edu.cn

***Abstract*—The default pulse shaping filter in the conventional multiple-input and multiple-output (MIMO) based orthogonal frequency division multiplexing (OFDM) system is a rectangular function, which unfortunately is highly sensitive to frequency synchronization errors and the Doppler spread. Shaped OFDM is able to considerably alleviate the effect of inter-carrier interference (ICI) as well as reduce the out-of-band frequency leak. In this paper, we study various pulse shaping functions and investigate their efficacy for reducing the ICI in the space-time block coded MIMO-OFDM system. We compare a new shaping pulse termed harris-Moerder pulse with several other popular Nyquist pulses such as the raised-cosine pulse and better than raised-cosine pulse. Our simulation results confirm that pulse shaping using a suitable shaping function other than the default rectangular one can alleviate ICI and thus achieve better bit error rate (BER) performance. Furthermore, it is demonstrated that the harris-Moerder shaping pulse is the most successful one in suppressing ICI.**

***Index Terms*—Pulse shaping, inter-carrier interference (ICI) reduction, orthogonal frequency-division multiplexing (OFDM), multiple-input and multiple-output (MIMO), space-time coding, Rayleigh fading channel.**

I. Introduction

Orthogonal frequency-division multiplexing (OFDM) [1], [2] has become an attractive modulation technology with wide employment in a variety of current telecommunications standards such as asymmetric digital subscribe line (ADSL) for high-speed wired Internet access, digital audio broadcasting (DAB), and digital terrestrial TV broadcasting (DVB). More recently, OFDM has made remarkable inroads into current and future wireless standards, e.g., WLAN (IEEE 802.11a/g/n), WiMAX (IEEE 802.16), 3GPP long term evolution (LTE), and IMT-Advanced.

OFDM is essentially a block modulation technique, which converts a wideband frequency selective fading channel into a number of parallel narrowband orthogonal sub-carriers that experience only flat fading. The primary advantages of OFDM lies in its ability to cope with severe frequency-selective fading due to multi-path without complex equalization filters. OFDM is able to attain high frequency efficiency as opposed to conventional frequency-division multiplexing techniques by overlapping the orthogonal sub-carriers. However, this advantage comes at the expense of the sensitivity to frequency offset leading to inter-channel interference and hence performance degradation.

Meanwhile, multiple-antenna technology, also dubbed multiple-input and multiple-output (MIMO), is emerging as an enabling technique to achieve high data rate and spectral efficiency by simultaneously transmitting parallel data streams over multiple antennas [3], [4]. The essential idea behind MIMO technology is space-time signal processing in which both the time and spatial dimensions are exploited through the use of multiple spatially distributed antennas. As such, a MIMO system effectively transforms multi-path propagation, traditionally treated as a nemesis for wireless communications, into user benefits.

The inaugural concept of MIMO was pioneered in Bell Labs in middle 1990s. Telatar studied MIMO system capacity under Gaussian channels in 1995 [5], while Foschini invented the layered space-time architecture in 1996 [6]. To realise the enormous capacity of MIMO systems, Wolniansky established the world's first MIMO testbed based upon the vertical Bell Laboratories layered space-time (V-BLAST) algorithm in 1997 [8], which achieved unprecedented spectral efficiency of 20-40 bit/s/Hz in indoor rich scattering propagation environments. V-BLAST breaks input data into parallel sub-streams that are transmitted through multiple antennas [6], [7], [9]. The astonishingly high spectral efficiency stem from parallel signal transmission resulting in remarkable spatial multiplexing gains. Another important category of MIMO techniques that strive to maximize diversity gains in lieu of rate increase is termed space-time coding, including space-time block codes (STBCs) [10], [11] and space-time trellis codes (STTCs) [12]. The third type of MIMO technology exploits channel state knowledge at the transmitter side through decomposing the channel coefficient matrix using singular value decomposition (SVD). The decomposed unitary matrices via SVD can be used to configure pre- and post-filters at the transmitter and receiver to achieve near optimum MIMO capacity [4].

MIMO and OFDM technologies can be used in conjunction to provide broadband wireless services for future fourth-generation (4G) wireless communications systems [13]. For a wideband MIMO channel whose fading is frequency selective, the complexity of optimum maximum likelihood (ML) MIMO detection grows exponentially with the product of the bandwidth and the delay spread of the channel. To this end,

MIMO-OFDM is preferred over MIMO-SC (single-carrier) in that OFDM modulation is employed to overlay on MIMO so as to convert a frequency-selective MIMO channel into multiple flat fading subchannels. MIMO-OFDM can be implemented as space-time coded OFDM (ST-OFDM), space-frequency coded OFDM (SF-OFDM), or space-time-frequency coded OFDM (STF-OFDM) [14]. In this paper, we restrict our system model to ST-OFDM as the focus of the paper is on reducing inter-carrier interference (ICI) using pulse shaping in MIMO-OFDM.

In a MIMO-OFDM system, inter-symbol interference (ISI) caused by multi-path propagation (time dispersion) can be eliminated by adding a frequency guard interval dubbed the cyclic prefix (CP) between adjacent OFDM symbols. However, the CP offer no resilience against frequency dispersion, where carrier frequency offset is introduced due to the Doppler spread. This causes a loss of orthogonality between the sub-carriers, and thus results in ICI. The frequency-localization of the pulse shaping filter in the MIMO-OFDM system plays a critical role in alleviating the sensitivity to frequency offset and thus reducing ICI caused by the loss of orthogonality. Another important benefit of pulse shaping is to reduce out-of-band frequency leak and hence increase spectral efficiency. For conventional MIMO-OFDM systems, the pulse shaping filter is a rectangular function, which exhibits a poor frequency decay property, and is thus highly sensitive to frequency synchronization errors and Doppler spread. This observation has motivated recent studies on the design of better pulse shaping functions for OFDM.

Shaped OFDM can reduce the effect of single tone interference such as produced by an in-band jammer. If an interfering signal has an integer number of cycles per OFDM frame interval, it will interfere only with one sub-carrier. However, if the interfering signal has a non-integer number of cycles, it will contribute a component to every OFDM sub-carrier. Therefore, a jammer within the OFDM band could project into all OFDM sub-carriers due to the side lobes of the $sinc(x)$ frequency response. However, using pulse shaping the interference could be isolated to a few OFDM channels by suppressing the side lobes with an appropriate window to filter the basis signal set [15].

Pulse shaping in MIMO-OFDM aims to replace the basic rectangular pulse which performs poorly in dispersive channels. Unfortunately, while the majority of work on MIMO-OFDM has been focused on the system design, and channel estimation and synchronization, limited research to date has been dedicated to this important niche area of research for MIMO-OFDM. Several approaches to pulse shaping for OFDM systems have been tried including Hermite waveforms [16] and Weyl-Heisenberg (or Gabor) frames [17]. In [18], the authors examined the use of pulse shaping to reduce the sensitivity of OFDM to carrier frequency offset. Several pulse shaping filters such as the rectangular pulse, raised-cosine pulse and the so-called "better than" raised-cosine pulse [19] were compared in [20]. The authors advocated that the "better than" raised-cosine pulse gave the best performance in the reduction of ICI. The effects on ICI reduction of several widely used Nyquist pulses including the Franks pulse, the raised-cosine pulse, and the "better than" raised-cosine pulse were compared in [24]. The Franks pulse [25] was reported to give the best performance. In [21], a new pulse shape was proposed and compared against Nyquist-I pulses [22]. Improved performance results for the proposed pulse shape were reported. Most recently, another new pulse termed the sinc with modified phase was proposed to reduce ICI in OFDM systems in [23].

In this paper, we investigate the effect of impulse shaping on ICI reduction for the space-time block coded MIMO-OFDM communications system. Although the above studies have reported results on the performance of various shaping pulses on the resistance to carrier frequency offset in OFDM systems, to the best of our knowledge, we are unable to find any published work on pulse shaping for MIMO-OFDM systems in the literature to date. More importantly, we will investigate the performance of a new shaping pulse dubbed the harris-Moerder pulse [26] on ICI reduction in coded MIMO-OFDM systems. We will present simulation results using various OFDM pulse shapes in different time-varying wireless fading channels, showing, among other things, how the channel model used has a significant effect on the final bit error rate (BER). Our comparative studies demonstrate that the harris-Moerder pulse outperforms other popular Nyquist pulses.

The remainder of this paper is organized as follows. Section II describes the software defined modules of the transceiver. Section III describes the various channel models used. Section IV describes the pulse shapes transmitted. Section V presents the bit error rate results obtained in the simulation, while in Section VI conclusions are presented for further research.

II. MIMO-OFDM Transceiver Model

A. System Model

In this paper, we consider the space-time block coded MIMO-OFDM communications systems. The transceiver architecture of the system is illustrated in Fig. 1. As can be observed from the figure, the MIMO-OFDM transceiver is comprised of the quadrature phase shift keying (QPSK) modulator, the space-time block coding component over OFDM with a cyclic prefix, the interleaver and block coding transmitting through various terrestrial Rayleigh fading channels. The system is able to achieve diversity gains in the space, time and frequency domains as well as coding gains from the interleaving and block coding. SBTC is implemented using the well-known *Alamouti* scheme [10] with two transmit and two receive antennas.

For the MIMO-OFDM transceiver model depicted in Fig. 1, denote by N_T, N_R, and N the number of transmit and receive antennas, and the number of sub-carriers, respectively. For the Alamouti scheme, we have $N_T = N_R = 2$.

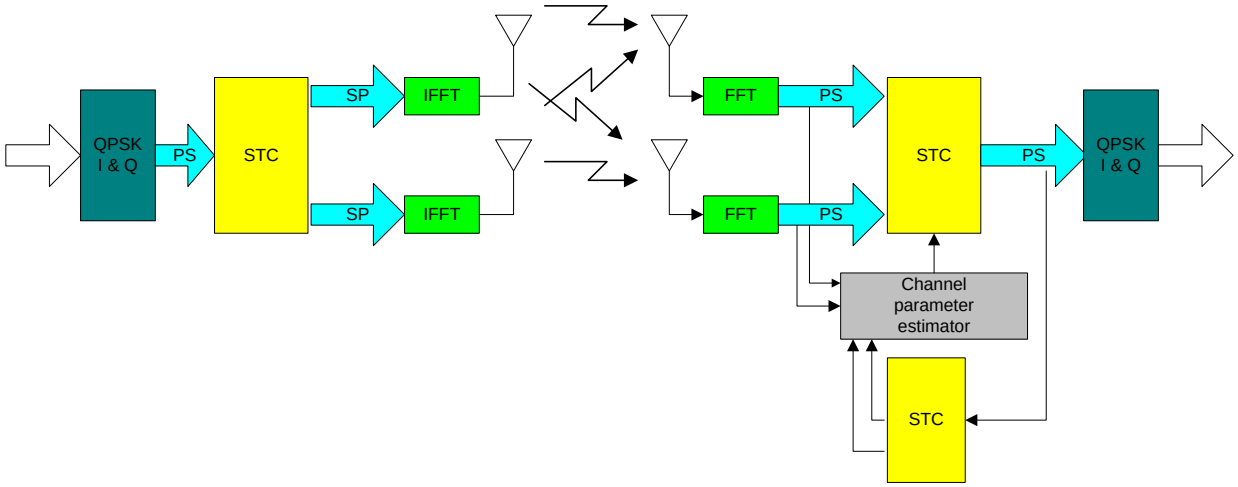

Fig. 1. Transceiver block diagram for the space-time block coded MIMO-OFDM communications system.

B. ICI Analysis

For the system model shown in Fig. 1, the complex envelope of the N-subcarrier OFDM block with pulse shaping sent through the ith transmit antenna can be expressed as

$$x_i(t) = e^{j2\pi f_c t} \sum_{k=0}^{N-1} d_{i,k} p(t) e^{2\pi f_k t} \tag{1}$$

where j is the imaginary unit, f_c is the carrier frequency, f_k is the sub-carrier frequency of the kth sub-carrier, $p(t)$ is the time-limited pulse shaping function, and $d_{i,k}$ is the data symbol sent through the kth sub-carrier of the ith transmit antenna, where $i = 1, 2, \cdots, N_T$, and $k = 0, 1, \cdots, N$. The data symbol $d_{i,k}$ is assumed uncorrelated with zero mean and normalized average symbol energy

$$E[d_{i,k} d_{i,m}^*] = \begin{cases} 1, & k = m \\ 0, & k \neq m \end{cases} \tag{2}$$

where * denotes the complex conjugate operator.

To ensure that the sub-carriers are mutually orthogonal, the following relationship must hold

$$\int_{-\infty}^{+\infty} p(t) e^{j2\pi f_k t} e^{-j2\pi f_m t} dt = \begin{cases} 1, & k = m \\ 0, & k \neq m. \end{cases} \tag{3}$$

Equation (3) implies that the Fourier transform of the pulse shaping function $p(t)$ must have spectral nulls to guarantee orthogonality at the frequencies of $f_k = \pm kW/N$, where W is the total available bandwidth, and $k = 1, 2, \cdots, N$.

It is well known that wireless fading channel distortion and the crystal oscillator frequency mismatch between the transmitter and receiver will introduce the carrier frequency offset $\triangle f$ and the phase error θ. Consequently, this introduces a multiplicative factor at the OFDM receiver. As a result, the received signal is expressed as [20]

$$r(t) = e^{(j2\pi \triangle f t + \theta)} \sum_{k=0}^{N-1} d_k p(t) e^{2\pi f_k t}. \tag{4}$$

Note that the transmit antenna index i is dropped in the above equation for ease of exposition.

The output from the mth sub-carrier correlation demodulator is given as

$$\begin{aligned} \hat{d}_m &= \int_{-\infty}^{+\infty} r(t) e^{-j2\pi f_m t} dt \\ &= d_m e^{j\theta} \int_{-\infty}^{+\infty} p(t) e^{j2\pi \triangle f t} dt \\ &\quad + e^{j\theta} \sum_{\substack{k=0 \\ k \neq m}}^{N-1} d_k \int_{-\infty}^{+\infty} p(t) e^{j2\pi (f_k - f_m + \triangle f) t} dt. \end{aligned} \tag{5}$$

With some further mathematical manipulation, the average ICI power for the mth data symbol can be shown as [20]

$$\bar{\sigma}_{\text{ICI}}^m = \sum_{\substack{k=0 \\ k \neq m}}^{N-1} \left| P\left(\frac{k-m}{T} + \triangle f \right) \right|^2 \tag{6}$$

where $P(f)$ is the Fourier transform of the pulse function $p(t)$. Denote by $\bar{\gamma}_{\text{SIR}}$ the ratio of the average signal power to average ICI power ratio, which can be obtained as

$$\bar{\gamma}_{\text{SIR}} = \frac{|P(\triangle f)|^2}{\sum_{\substack{k=0 \\ k \neq m}}^{N-1} \left| P\left(\frac{k-m}{T} + \triangle f \right) \right|^2}. \tag{7}$$

It is evident from (6) that the average ICI power for the mth symbol average across different sequences is contingent on the number of sub-carriers N and the spectral magnitudes of $P(f)$ at the frequencies of $((k-m)/T + \triangle f), k \neq m, k = 0, 1, \cdots, N-1$.

As indicated in (3), $P(f)$ is designed to have spectral nulls at the frequency points of $(k-m)/T$. Therefore, (6) is evaluated to zero providing $\triangle f = 0$. However, we have $\triangle f \neq 0$ under realistic channels. The focus of our research is to find a new pulse shaping function which is able to minimize (6).

III. Pulse Shapes

The data pulse input into the inverse fast Fourier transform (IFFT) modulator, and transmitted as a complete pulse on one sub-carrier, has a very large bandwidth due to the steep edges of the square pulse [2]. The data pulse can be shaped to reduce the side lobes, which then also reduces the amount of energy transmitted out of band and the resultant channel effects. This is termed *shaped* OFDM.

Shaped OFDM can reduce the effect of single tone interference such as produced by an in-band jammer. If an interfering signal has an integer number of cycles per OFDM frame interval it will interfere only with one subcarrier, however if the interfering signal has a non-integer number of cycles it will contribute a component to every OFDM sub-carrier. Therefore a jammer within the OFDM band could project into all OFDM sub-carriers due to the side lobes of the $sinc(x)$ frequency response, however using pulse shaping the interference could be isolated to a few OFDM channels by suppressing the side lobes with an appropriate window to filter the basis signal set.

One measure of success of a specific pulse shape is how much it reduces the spectral side lobes of the transmitted signal. The other main cause of degradation in OFDM is the ICI between sub-carriers, which can also be reduced with pulse shaping. The shaping also introduces controlled ISI at times other than the samples taken during the receiver decision times.

Another major advantage of shaping the OFDM signal is to reduce sensitivity to carrier frequency offset errors due to a time varying channel and Doppler effects, thereby destroying the orthogonality between channels. The most common rectangular pulse $p_{\text{rec}}(t)$, expressed as follows, does not offer robustness even to modest frequency offset.

$$p_{\text{rec}}(t) = \begin{cases} \frac{1}{T}, & -\frac{T}{2} \leq |t| \leq \frac{T}{2} \\ 0, & \text{otherwise.} \end{cases} \quad (8)$$

Some simulation work has showed that in an OFDM system even a simple Gaussian shaped pulse, with a spread width of 10% of the symbol time, will reduce the sensitivity of the system to a frequency offset by a factor of almost 6 dB [28].

An additional advantage of shaping is that an interfering tone in the frequency band of the OFDM sub-carriers may interfere with all the sub-carriers however the interference may be isolated to a few sub-carriers by replacing the square envelope with a shaped envelope. The envelope can be a standard window or the impulse response of a low pass filter applied to the basis signal set.

Pulse shaping can be then be done with polyphase filters. A window shaped envelope has high adjacent ICI and low ISI, while a filter shaped envelope has high ISI and low adjacent ICI, allowing a trade-off between the two by shaping the filter accordingly. Equalization can be added after the IFFT or polyphase filter to suppress the interference and decouple the adjacent channels and time frames

In this section, we compare five different shaping pulses. We start with the classic raised-cosine pulse, which although does reduce side lobes but is not the optimum pulse shape. A greater side lobe suppression can be obtained with a "better than raised-cosine pulse" as described in [20]. The third and fourth pulse shapes tested are the *duo-binary* pulse and the *triangular* pulse. The last shaping pulse introduced is the recently proposed *harris-Moerder* window [15], which is a modified square root Nyquist pulse using a *harris taper*. It will be demonstrated with simulation results present in Section V that the harris-Moerder pulse is the best performing shaping pulse in the sense of reducing ICI and achieving the best BER performance for the shaped MIMO-OFDM system.

A. Raised-Cosine Pulse

A commonly used pulse shape is the raised-cosine pulse, i.e., the frequency domain reciprocal of the time domain Nyquist pulse, which significantly suppresses spectral re-growth (side lobes) and ICI. When side lobes are suppressed the width of the pulse is increased.

The time domain expression of the raised-cosine pulse shaping function denoted as $p_{\text{rc}}(t)$ is given at the bottom of the next page, where α is the roll-off factor, and $0 \leq \alpha \leq 1$. As α approaches to zero, the pulse shape becomes closer to a rectangular.

Let $P_{\text{rc}}(f)$ represent the Fourier transform of the raised-cosine pulse. The time and frequency representations $p_{\text{rc}(t)}$ and $P_{\text{rc}}(f)$ of the raised-cosine pulse are shown in Fig. 2.

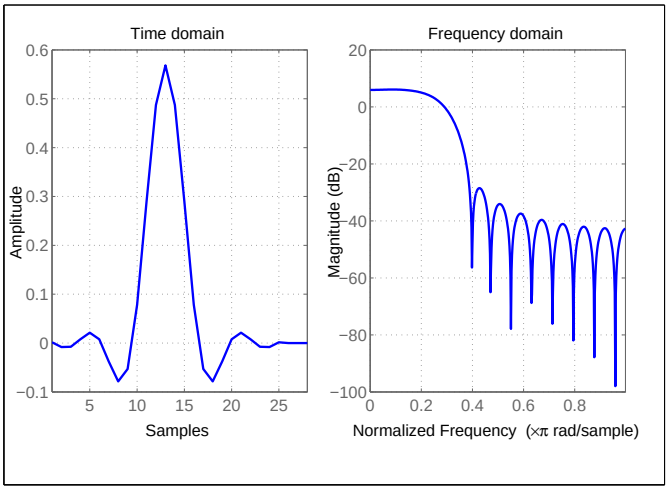

Fig. 2. Time and frequency domain representation of the raised-cosine pulse.

B. Better Than Raised Cosine Pulse

Recently, a new shape of pulse has been discovered that can increase the BER performance of the OFDM system [19], including reducing even further the ICI [20]. This pulse shape has been termed the *better than raised cosine* (BTRC) pulse. The mathematical expression for the time domain representation of the BTRC pulse is given at the bottom of the next page.

Fig. 3 shows the time domain representation of the pulse for three different values of α. At an α of 0.5, the BTRC

pulse samples are divided into three parts equally between the leading edge, the flat top and the trailing edge. At an α of 0m the BTRC pulse becomes a square wave. It can be observed that the BTRC pulse requires a large number of samples to achieve leading and trailing edges with detailed shape, and most of these samples are in the flat top. It is noted that both the raised-cosine and BTRC pulses collapse the rectangular pulse. The normalized frequency response of the BTRC pulse at $\alpha = 1$ is shown in Fig. 4.

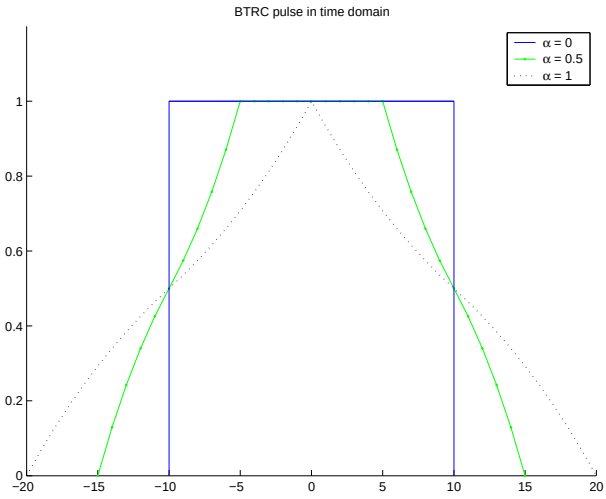

Fig. 3. Time domain representation of the better than raised-cosine pulse with three different α values.

Experimental and theoretical results indicate that $p_{\text{btrc}}(t)$ outperforms the rectangular and raised-cosine pulses in the reduction of the average ICI power. Calculations show that for a minimum average signal power to ICI ratio (SIR) of 25 dB, when using the raised-cosine pulse, the normalized frequency offset must be less than 0.1052. In contrast, the tolerable normalized frequency offset may be as large as 0.1844 when one uses the BTRC pulse.

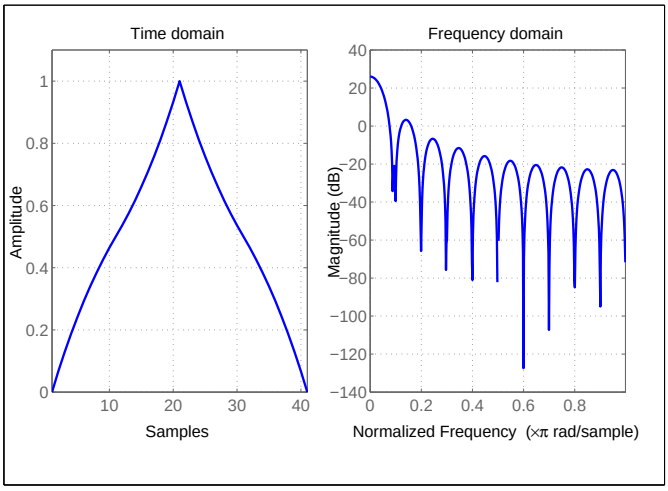

Fig. 4. Time and frequency domain representations of the better than raised-cosine pulse at $\alpha = 1$.

C. Duo-Binary

The duo-binary pulse is designed to minimize ISI in a band-limited channel (all real channels are band limited). This shape where controlled ISI is introduced is classified as a *partial response signal*. Its spectrum decays to zero smoothly [29].

The duo-binary pulse shape is given as follows

$$x(t) = sinc(2Wt) + sinc(2Wt - 1) \tag{11}$$

where W is the bandwidth and the $sinc$ function is defined as $\sin(x)/x$. A symbol rate of $2W$, being the Nyquist rate, is achieved thereby giving greater bandwidth efficiency compared to the raised cosine pulse.

The properties of this pulse can be further enhanced by precoding the signal using modulo two subtraction on the original data sequence to prevent error propagation during detection.

D. Triangular Pulse

Using an up-sampling rate of four samples on the BTRC pulse has the effect of reducing it to a triangular shape with

$$p_{\text{rc}}(t) = \begin{cases} \dfrac{1}{T}, & 0 \le |t| \le \frac{T(1-\alpha)}{2} \\ \dfrac{1}{2T}\left\{1 + \cos\left[\dfrac{\pi}{\alpha T}\left(|t| - \dfrac{T(1-\alpha)}{2}\right)\right]\right\}, & \frac{T(1-\alpha)}{2} \le |t| \le \frac{T(1+\alpha)}{2} \\ 0, & \text{otherwise.} \end{cases} \tag{9}$$

$$p_{\text{btrc}}(t) = \begin{cases} \dfrac{1}{T}, & 0 \le |t| \le \frac{T(1-\alpha)}{2} \\ \dfrac{1}{T} e^{\left(\frac{-2ln2}{\alpha T}\left(|t| - \frac{T(1-\alpha)}{2}\right)\right)}, & \frac{T(1-\alpha)}{2} \le |t| \le \frac{T}{2} \\ \dfrac{1}{T}\left\{1 - e^{\left(\frac{-2ln2}{\alpha T}\left(\frac{T(1+\alpha)}{2} - |t|\right)\right)}\right\}, & \frac{T}{2} \le |t| \le \frac{T(1+\alpha)}{2} \\ 0, & \text{otherwise.} \end{cases} \tag{10}$$

values of 0, 0.5, 1, 0.5, 0.

E. harris-Moerder Pulse

An improvement on the standard root raised-cosine (RRC) filter is the recently proposed harris-Moerder pulse [26]. This is an improved Nyquist pulse that reduces ISI by eliminating distortion associated with truncation of the standard RRC filter impulse response. The pulse is generated using the Parkes-McClelllan (or Remez) algorithm [26].

A comparison of the harris-Moerder pulse, using 20 symbols in the filter and specifying equi-ripple side lobes, with the standard root raised-cosine filter, is shown in Fig. 5.

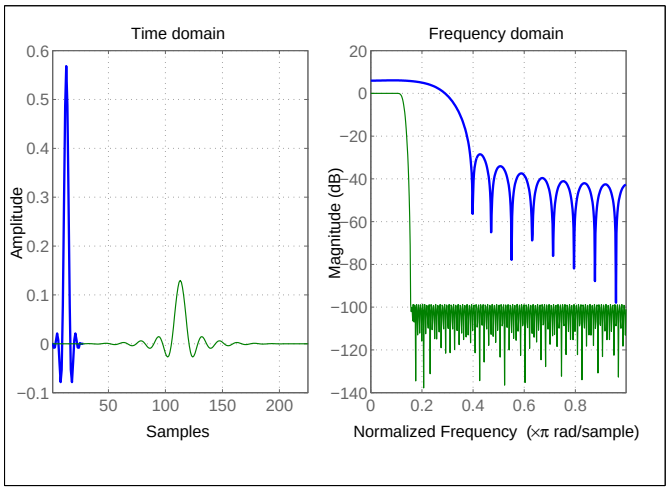

Fig. 5. Comparison of the harris-Moerder pulse (20 symbols, equiripple side lobes, green pulse on right) with a root raised cosine filter (left pulse in blue).

As will be shown in Section V, the harris-Moerder pulse will remarkably reduce ICI and thus improve the BER performance of the MIMO-OFDM system in comparison with other shaping pulses.

F. Equalization

ISI is caused by both channel distortion, which varies with time, and the overlapping raised cosine signal pulses after the receiver filter, which is a fixed amount set by the transmitter and receiver filters. The signal can be therefore be described by three components as follows

$$y_k = a_k + \sum_{\substack{n=0 \\ n \neq k}}^{\infty} a_n x_{k-n} + n_k \qquad (12)$$

where a_k represents the desired information symbol at the kth sampling instant, and n_k is the noise at the kth sampling instant. The middle term on the right hand side of (12) is the ISI term.

The fixed ISI renders the signal virtually unintelligible and needs to be removed. The simplest method to remove this fixed ISI is with a standard zero-forcing equalizer (ZFE). However, a ZFE equalizer has the serious disadvantage of amplifying noise. A minimum mean square error (MMSE) equalizer that tolerates a specified amount of ISI is used in the simulations as will be presented in Section V.

IV. Terrestrial Fading Channel Models

As aforementioned, the wireless fading channel in conjunction with pulse shaping has a considerable influence on the performance of the MIMO-OFDM communications system. In this section, we look into various terrestrial air channel models.

Terrestrial radio reception normally suffers degradation by fading due to multi-path reception of reflected signals that result in statistical cancelation or addition of the received signal. For simplicity, a radio channel is often modeled as a flat fading channel with independent identically distributed (i.i.d.) complex Gaussian coefficients. However, real channels are not so simple and the un-modeled parameters can have significant positive or negative effects depending upon the characteristics of the signal transmitted.

In a wireless fading channel with additive white Gaussian noise (AWGN), signals that do not include a direct path component follow a Rayleigh distribution, which means the square of the path gains are exponentially distributed. A Rayleigh distribution is therefore a more realistic air channel model than a basic Gaussian model.

The Rayleigh distribution is a specific case of the two parameter Weibull distribution [30]

$$f(T) = \beta/\eta \, (T/\eta)^{\beta-1} \, e^{-(T/\eta)^{\beta}} \qquad (13)$$

where the shape or slope parameter β equals two, and the scale parameter η is variable. As the ratio of the LOS signal power over the multi-path signal power increases (called the K factor), the Rician distribution tends to an AWGN distribution. As the ratio decreases, the Rician tends towards the Rayleigh distribution.

When the bandwidth of the transmitted signal is narrow enough to be within the coherence bandwidth, where all spectral components of the transmitted signal are subject to the same fading attenuation, then this ideal case is described as a flat fading channel. A channel is *slow fading* if the symbol period is much smaller than the coherence time, and *quasi-static* if the coherence time is in the order of a "block interval".[1]

It is obviously easier to compensate for fading in a flat channel than the one where fading is non-linear. Diversity techniques over fading channels non correlated in time, frequency and space are used to reduce the effects of fading and therefore improve the spectral efficiency of the air channel.

The following wireless fading channel models are used in our simulations.

A. Jakes Model

Practical models for mobile communications assume there are many multi-path components and all have the same Doppler spectrum with each multi-path component being itself

[1]It is noted, however, that different authors use considerably different definitions of a "block", some mean no fading over one whole transmitted frame while others mean over either one or even two sampled symbol periods. The simulation results in this work assume constant fading over one symbol period.

the sum of multiple rays. The first model to take into account both Doppler effects and amplitude fading effects was devised by Jakes in 1974 [31].

The Doppler effect of a moving receiver is described by the classical Jakes spectrum, which gives a "bathtub" shape of signal power against velocity, with singularities at the minimum and maximum Doppler frequencies. The basic Jakes channel fading model incorporating this Doppler shift simulates time correlated Rayleigh fading waveforms.

The model assumes that N equal strength waves arrive at a moving receiver with uniformly distributed angles, coming from 360° around the receiver antenna, as illustrated in Fig. 6. The fading waveforms can therefore be modeled with $N+1$ complex oscillators. This method, however, still creates unwanted correlation between waveform pairs.

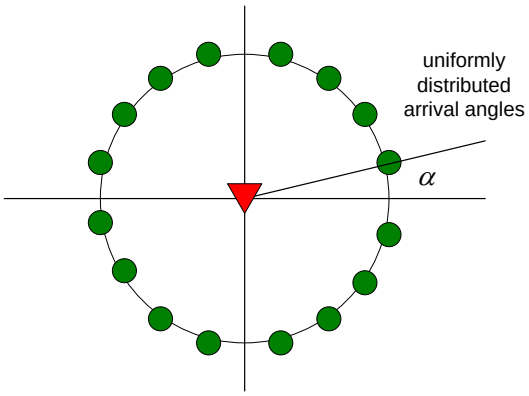

Fig. 6. Jakes model of multi-path interference.

B. Dent's Model

The unwanted correlation of Jake's model is removed in a modification by Dent *et al*. The unwanted correlation can be corrected by using orthogonal functions generated by Walsh-Hadamard codewords to weigh the oscillator values before summing so that each wave has equal power [32]. The weighting is achieved by adjusting the Jake's model so that the incoming waves have slightly different arrival angles α_n.

The modified Jakes model is given by

$$T(t) = \sqrt{\left(\frac{2}{N_0}\right)} \sum_{n=1}^{N_0} \left[\cos(\beta_n) + i\sin(\beta_n)\right] \cos(\omega_n t + \theta_n) \tag{14}$$

where the normalization factor $\sqrt{(2/N_0)}$ gives rise to $E\{T(t)T^*(t)\} = 1$, $N_0 = N/4$, $i = \sqrt{(-1)}$, $\beta_n = \pi * n/N_0$ is phase, θ is initial phase that can be randomized to provide different waveform realisations, and $\omega_n = \omega_M \cos(\alpha_n)$ is the Doppler shift.

Dent's model successfully generates uncorrelated fading waveforms thereby simulating a Rayleigh multi-path air channel. The "bathtub" shaped power spectrum distribution (PSD) of Rayleigh fading based on Dent's model is estimated by the periodogram as shown in Fig. 7. For an input data stream $x(n)$ that is a zero-mean, stationary random process and its discrete Fourier transform (DFT) denoted by $X(w)$, the periodogram is defined as $I(w) = |X(w)|^2/N$, where N is the data length.

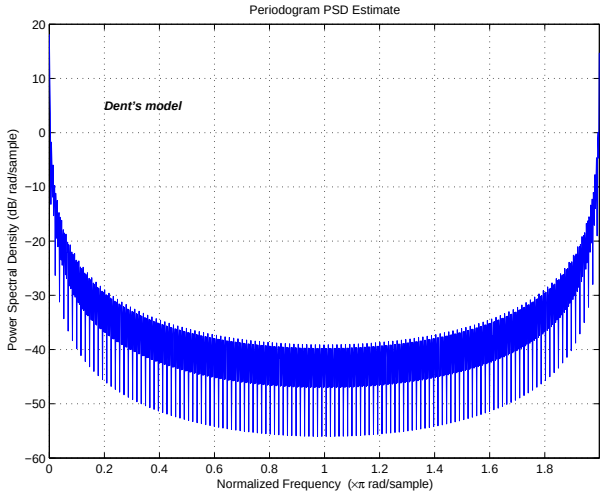

Fig. 7. Power spectrum distribution of Rayleigh fading using Dent's model.

C. Auto-regressive Model

Most fading models assume Rayleigh fading in an isotropic channel. However, this assumption is not always valid. In an attempt to add directional fading to the model, an autoregressive approach has been successfully developed in [33]. Furthermore, it has been proved that the classical Jakes model introduces fading signals that are not wide sense stationary, and the auto-regressive model remedies this shortcoming.

The periodogram of the autoregressive model, shown in Fig. 8, is still a "bath tub" shape, albeit with a narrower cut-off than Dent's model.

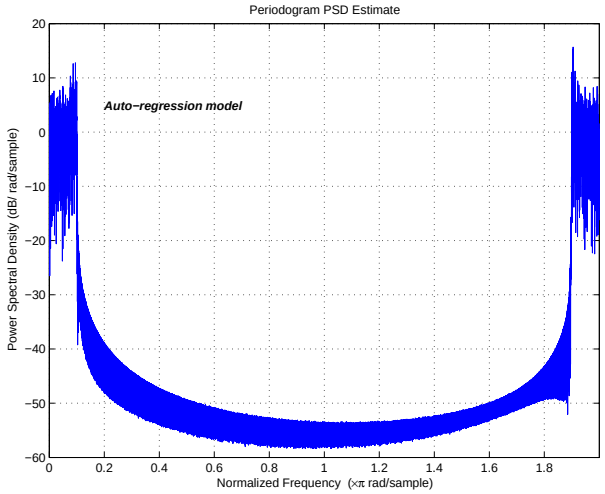

Fig. 8. Power spectrum distribution of Rayleigh fading using the auto-regressive model.

D. Stanford University Interim Models

For the purposes of the IEEE 802.16 standard on LAN/MAN air interfaces, the IEEE have adopted and modified a series of models called the Stanford University Interim (SUI) models [34]. These channel models for fixed wireless applications cover six scenarios of terrain and environment for the 1-4 GHz band.

The SUI models are different from the previous models since they assume time-variant (frequency-selective) channels. As a result, they need to be modeled with a *tapped delay line* in lieu of a more simple transfer function. Each tap represents the path of a different delayed frequency. Although there are theoretically an infinite number of frequencies, it has been found that modeling with three taps is accurate enough.

The SUI model differs from the simpler Rayleigh fading distribution in that it does not exhibit the typical Rayleigh PSD of the previous two models. The difference is most noticeable in the PSD estimate where the power spectral density at the high end of the spectrum does not increase asymptotically but instead tapers to zero forming a "half bathtub" shape, as shown in the periodogram Fig. 9.

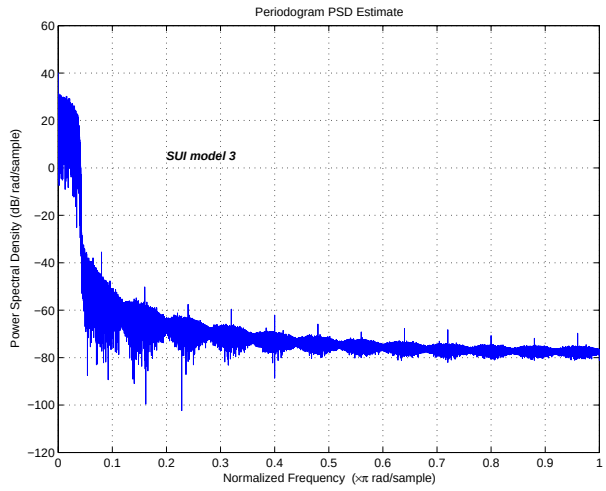

Fig. 9. SUI-3 PSD showing tapering at high frequency.

E. Tropospheric Model

The tropospheric (non-ionospheric) communications in the VHF (30 to 300 MHz) and UHF (300 MHz to 3 GHz) bands can cover several hundred kilometers. In these bands oxygen and water vapor absorb RF energy with the loss being dependent on frequency and atmospheric conditions such as humidity. The previous models would not be suitable for this environment. The frequency selective absorption characteristics can be modeled by a transfer function of the following form

$$H(f) = He^{j0.02096f[10^6+N(f)]l} \tag{15}$$

where $N(f)$ is the complex refractivity of the atmosphere in parts per million. The resulting channel model can be simulated using finite impulse response filtering techniques [35].

An example of a tropospheric model for microwave communication between fixed antenna towers is *Rummler's model*. This is a line of sight model with a very small number of multi-path components resulting in very slow fading [35].

The channel model becomes especially important in the case of designing MIMO algorithms since these are especially sensitive to the channel matrix properties. Some authors [36] caution that since results for realistic channels are still unknown the predicted gains of MIMO systems may be premature.

V. Simulation Results

In this section, we present experimental simulation results to demonstrate the performance improvements of shaping the coded MIMO-OFDM system using the various time-limited pulse shaping functions discussed in Section III. We will first show the the frequency responses of shaped OFDM sub-carriers using these shaping pulses, followed by the presentation of the BER curves to demonstrate the error performance of the MIMO-OFDM system over wireless fading channels.

A. System Configuration Parameters

The OFDM signals are generated with a 64-point IFFT, thereby givingv 64 sub-carriers conforming to the IEEE 802.11 standard. The baseband frequencies therefore range from 512 KHz to 32.8 MHz. Assuming a typical bandwidth of 16.56 MHz (as in 802.11a), the channel separation is $16.56/64 = 258.74$ KHz and the OFDM frame duration is 3.86 μs. To counter ISI, the cyclic prefix added is set at 25% of the OFDM block, thereby adding another 0.96 μs to the transmitted frame. The data bit frame length is 131072 bits, while the IQ symbol frame length is 524288.

Error detection and correction is performed by using a linear block coder of codeword length of 4 and parity length of 2. Optimum results for the MMSE equalizer are obtained experimentally by varying firstly the roll-off factor, a value of 0.495 is found optimum, and secondly varying the symbol noise power, a value of 6 is optimum. The optimum parameters are found by empirical try and error methods.

B. Frequency Spectrum of Shaped OFDM Signal

The frequency response of the OFDM sub-carrier signals at the transmitter after the IDFT modulation and shaping using a standard root raised-cosine filter is shown in Fig. 10. The filtered signal shows a sidelobe suppression of about 30 dB. At the receiver the signal was passed through a second root raised cosine pulse prior to input to the DFT demodulator. The resulting frequency response of a subcarrier is shown in Fig. 11.

The frequency response of the OFDM demodulated output, without shaping and with shaping using the raised-cosine pulse filter at the receiver *after* demodulation is shown in Figs. 12 and 13. With the shaped OFDM the 64 sub-carriers can clearly be seen approximately 20 dB above the noise, while in the unshaped signal, the subcarriers cannot be seen amongst the noise.

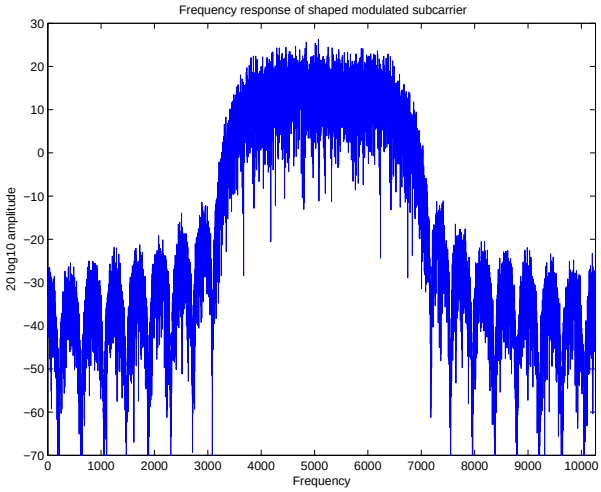

Fig. 10. Frequency response of the shaped OFDM signal at the transmitter using the root raised-cosine filter.

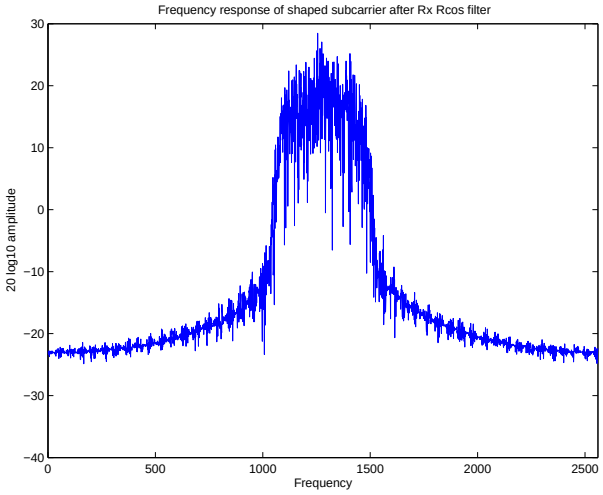

Fig. 11. Frequency response of the shaped OFDM signal after passing through the receiver root raised-cosine filter and before the the DFT.

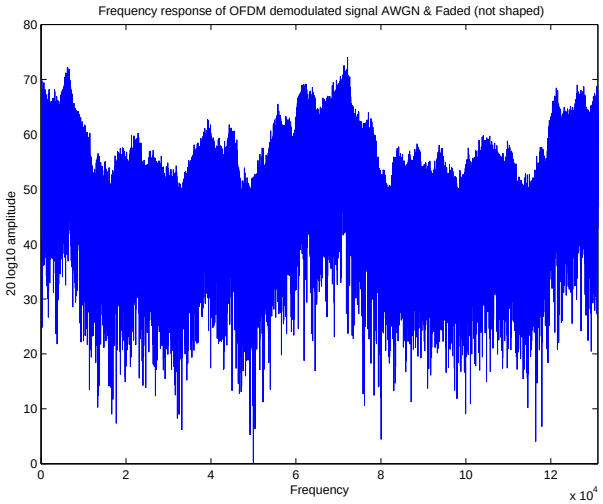

Fig. 12. Frequency response of demodulated (not-shaped) OFDM.

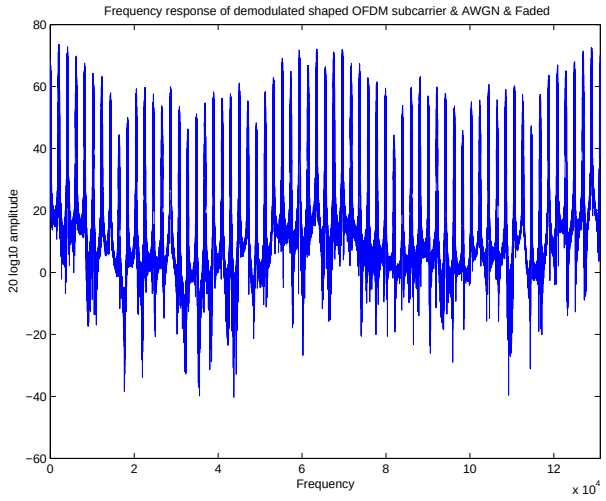

Fig. 13. Frequency response of demodulated shaped OFDM showing the sub-carriers.

The frequency response of an OFDM sub-carrier through a raised-cosine pulse is shown in Fig. 14, whereas the same pulse after equalization with five coefficients is shown in Fig. 15. The axes of the two plots are the same for comparison purposes. It can be observed how the MMSE equalization, using only five coefficients, suppresses the out of band sidelobes by about 40 dB.

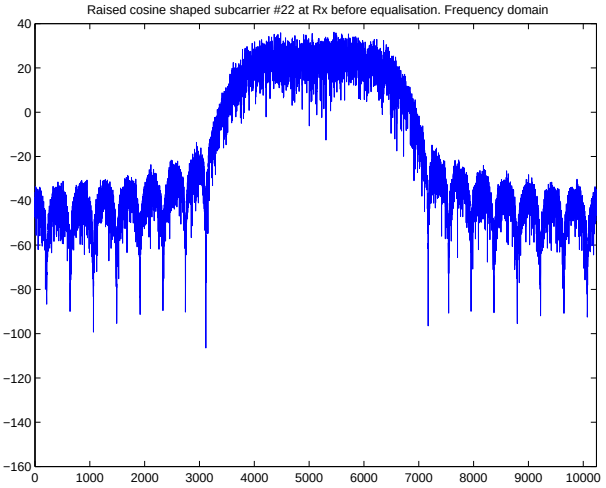

Fig. 14. Frequency response of raised-cosine shaped OFDM sub-carriers before equalization.

Figs. 16 and 17 show an OFDM sub-carrier shaped using the harris-Moerder pulse before equalization, and after equalization using seven equalization coefficients. The graphs have the same axis scales for comparison. The equalization can be seen to be very effective even though the MMSE equalizer uses less than half the number of coefficients as there are samples in the harrise-Moerder shaping pulse.

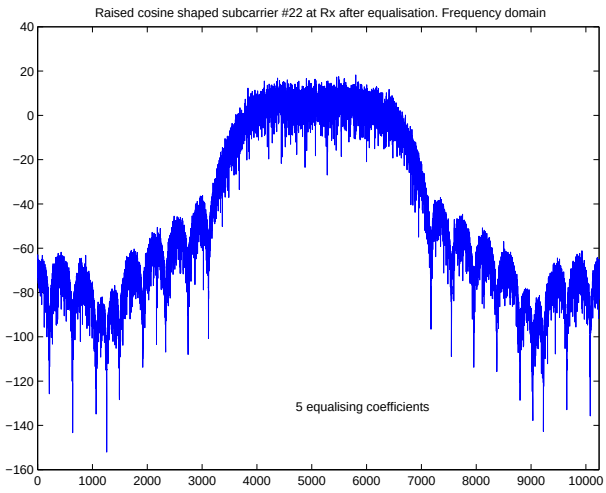

Fig. 15. Frequency response of raised-cosine shaped OFDM sub-carriers after equalization.

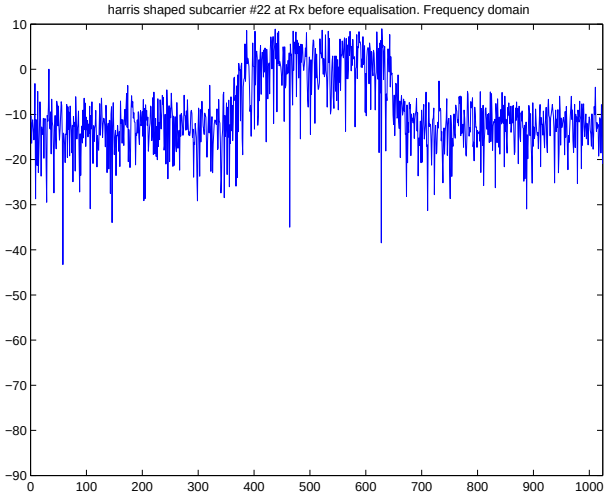

Fig. 16. OFDM sub-carrier no. 22 with `harris-Moerder` pulse (20 symbols, equi-ripple side lobes) before equalization.

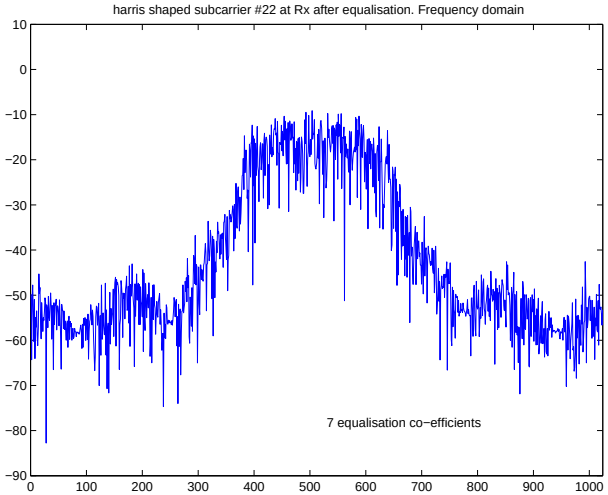

Fig. 17. `harris-Moerder` pulse equalized with seven coefficients (20 symbols, equiripple side lobes).

C. BER Performance Results

First of all, we plot several basic performance curves in Fig. 18 for the baseline MIMO-OFDM system using the Alamouti STBC scheme without pulse shaping.

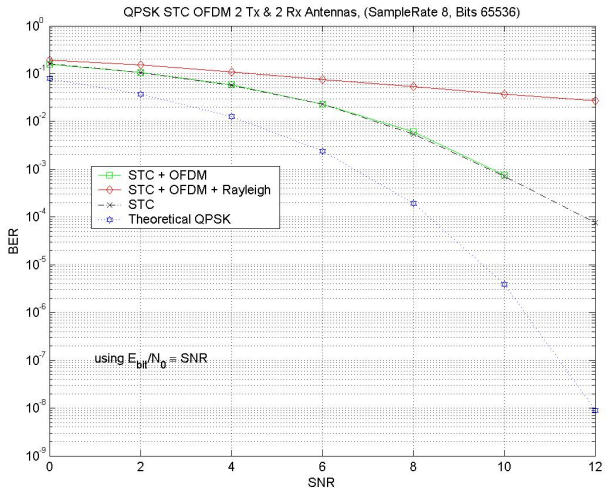

Fig. 18. Comparisons of the BER performance curves for STC, STC OFDM and STC OFDM under Rayleigh fading.

1) Raised Cosine and harris-Moerder Pulse Shaped OFDM: Shaping the OFDM pulse significantly improves the BER. As shown in Fig. 19, a Matlab designed raised cosine pulse, divided between the transmitter and receiver as root raised cosine filters, achieves about a 3 dB improvement over non shaped MIMO-OFDM. it can be seen that shaping with the harris-Moerder pulse at the transmitter increases the BER by more than 2 dB over raised cosine shaped MIMO-OFDM. The Rayleigh fading in these cases uses the auto-regressive model.

2) DuoBinary Pulse Shaped OFDM: The standard DuoBinary pulse, 61 samples long and equalised with the maximum number of coefficients (61) could not successfully be overlapped in the time domain when up-sampled by a factor of four. Fig. 20 shows the best results obtained, leveling out at an error rate of about 12% at an SNR around 6 dB.

Increasing the upsampling rate by double, to eight samples, gives better results, as shown in Fig. 21. However, curiously the BER curve for an AWGN channel follows the shape of a Rayleigh fading channel.

3) BTRC Pulse Shaped OFDM: The least successful pulse shape is the BTRC pulse. Equalisation is unsatisfactory, a greater upsampling rate is required than for other pulses meaning that it would be less practical to implement than other pulse shapes since sampling hardware would have to work at much higher speeds. Although this pulse shape was previously used successfully in OFDM to reduce the effects of unwanted frequency offset [37], the authors used an OFDM pulse length of the same length as the the BTRC pulse shaping filter. Additionally, since there was no time domain overlap there was no need to implement equalisation in their simulation.

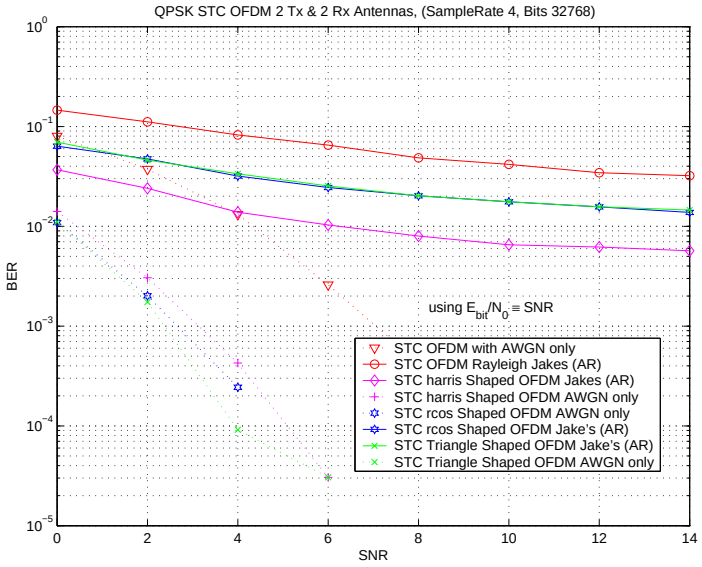

Fig. 19. Comparison of STC OFDM with AWGN only (not faded) with STC OFDM, STC Shaped OFDM (raised cosine), STC Shaped OFDM (harris-moerder) filter, equalized with 5 and 7 coefficients respectively, using the auto-regressive model of Rayleigh fading.

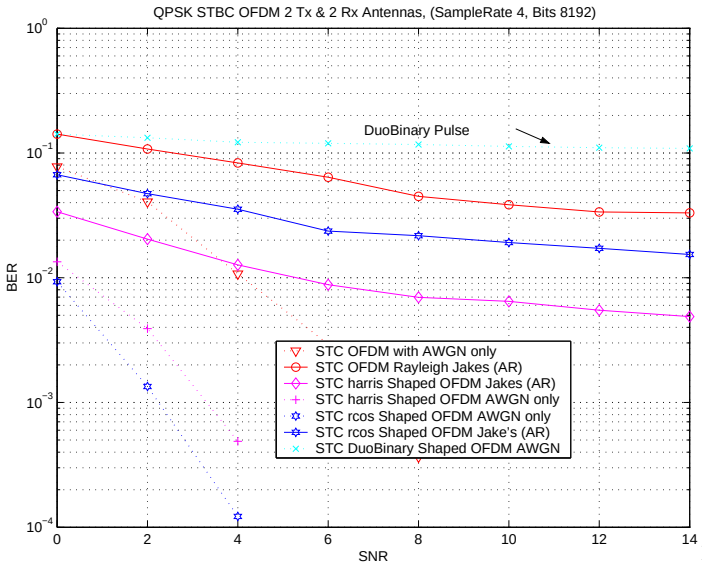

Fig. 20. DuoBinary pulse shaped OFDM with very high BER.

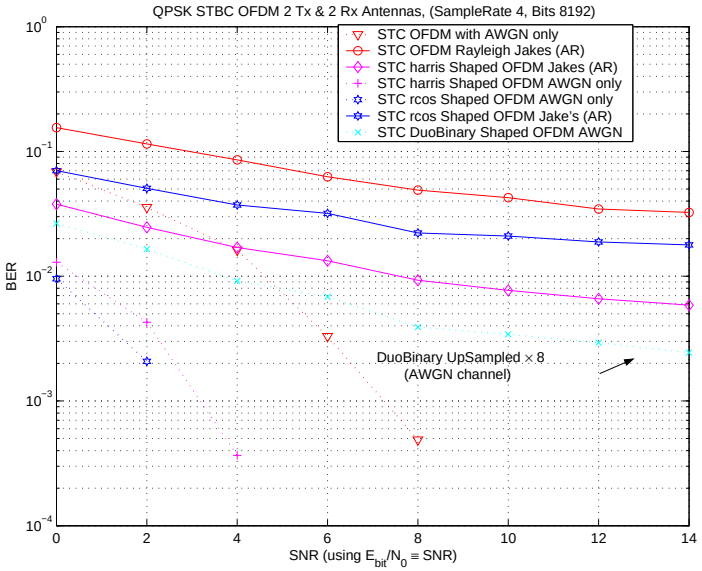

Fig. 21. DuoBinary pulse shaped OFDM upsampled by eight.

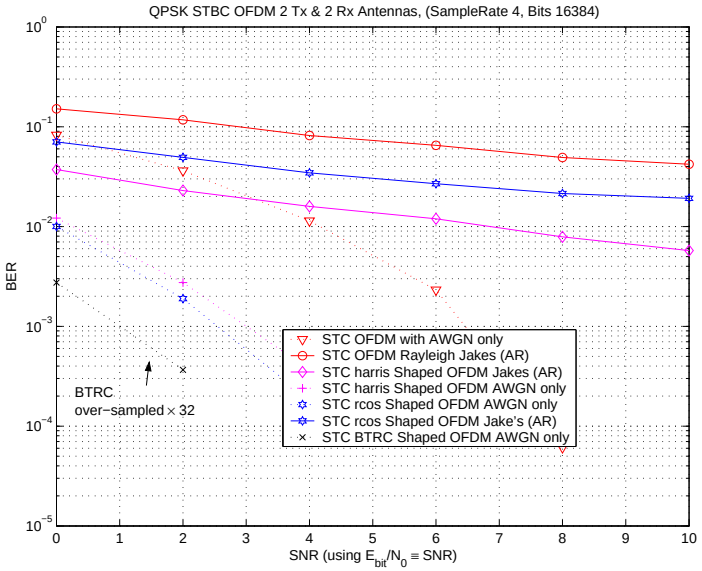

Fig. 22. Comparison of STC BTRC shaped OFDM (black line, alpha = 0.5 and upsampling by 32) with STC OFDM with AWGN only (not faded) with STC OFDM, STC shaped OFDM (raised cosine).

For an over-sampling of 8 and an α of 0.1 the BER curve still is not as good as unshaped STC OFDM in an AWGN channel. For the extreme case of an over sampling rate greater than the pulse width (therefore no time domain overlap) the BTRC gives the best results for an AWGN channel, as shown in Fig. 22. It should be noted that using the BTRC pulse in this manner is not a comparison under like conditions with the other modulation techniques.

4) Triangular Pulse Shaped OFDM: Modifying the BTRC pulse by truncating the long flat top of the pulse, and up-sampling at a rate four, inadvertently produced a triangular wave with values [0 0.5 1 0.5]. The BER of the triangular pulse were very similar to the raised cosine pulse at this sample rate, as shown in Fig. 23.

Not all possible variations of pulse shapes and equalisation parameters under different fading environments have been tested here. There may be versions that are optimised under some circumstances and not under others.

VI. Conclusions

In this paper, we investigate the efficacy of impulse shaping in reducing the ICI for the space-time block coded MIMO-OFDM communications system. Little existing work is known about the influence of pulse shaping for space-time coded

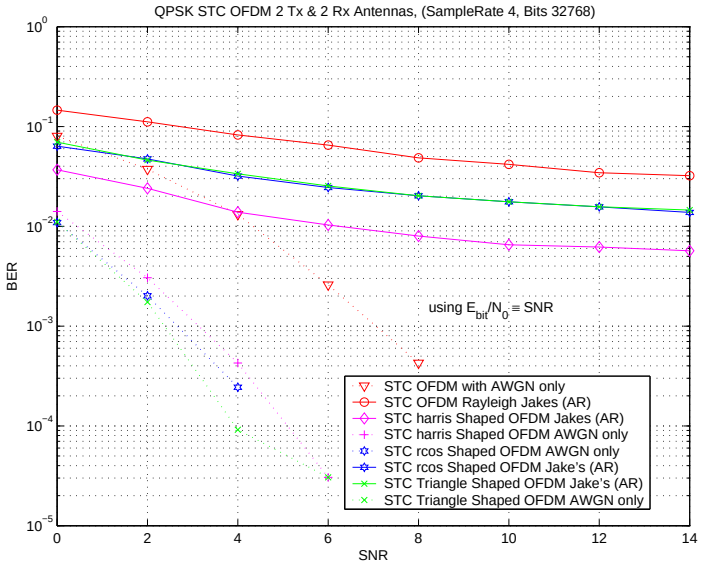

Fig. 23. Comparison of STC OFDM, STC shaped OFDM (raised cosine), STC Triangular shaped OFDM, STC shaped OFDM (harris-moerder), (under both AWGN and Jake's auto-regressive model of Rayleigh fading.

MIMO-OFDM systems. This work studies various shaping pulses and reports on their effect on alleviating the ICI for the MIMO-OFDM system. More importantly, we investigate the shaping performance of the new harris-Moerder pulse.

Simulation results are presented to demonstrate that shaping the OFDM pulse significantly improves on the system BER performance. Our results clearly indicate that the new harris-Moerder pulse outperforms other popular Nyquist pulses in the sense of improve the BER of the OFDM system. Moreover, the underlying channel model used has a significant effect on the BER.

The system could most likely be improved by adding further features, albeit at a cost of increasing the computational complexity. The optimum number of equalisation coefficients for each shape still needs to be determined. Adaptive pulse shaping by varying the parameters of the pulse shapes could also be explored for optimum performance in a time variant channel.

ACKNOWLEDGEMENT

We are grateful to Professor fred harris (sic) at San Diego State University for his assistance with the *harris-Moerder* pulse shape in this work.

This work is partly supported by the *International Science Linkages* established under the Australian Government's innovation statement *Backing Australia's Ability*.

REFERENCES

[1] J. Russell and W. Xiang, "Pulse shaping in MIMO COFDM over Rayleigh fading channels," in *Proc. International Conference on Wireless and Mobile Communications (ICWMC'09)*, Cannes, France, Aug. 2009, pp. 174-178.

[2] R. Prasad, *OFDM for Wireless Communications Systems*, Boston, M.A., Artech House, 2004.

[3] D. Gesbert, M. Shafi, D-S. Shiu, P. J. Smith, and A. Naguib, "From theory to practice: An overview of MIMO space-time coded wireless systems," *IEEE J. Sel. Areas Commun.*, vol. 21, no. 3, pp. 281-302, Apr. 2003.

[4] A. J. Paulraj, D. A. Gore, R. U. Nabar, and H. Bolcskei, "An overview of MIMO communications - a key to gigabit wireless," *Proc. IEEE*, vol. 92, no. 2, pp. 198-218, Feb. 2004.

[5] E. Telatar, "Capacity of multi-antenna Gaussian channels," *European Transactions on Telecommunications*, vol. 10, no. 6, pp. 585-595, Nov./Dec. 1999.

[6] G. J. Foschini, "Layered space-time architecture for wireless communication in a fading environment when using multi-element antennas," *Bell Labs Tech. J.*, vol. 1, no. 2, pp. 41-59, Autumn 1996.

[7] G. D. Golden, G. J. Foschini, and R. A. Valenzuela, "Detection algorithm and initial laboratory results using V-BLAST space-time communication architecture," *Electronics Letters*, vol. 35, no. 1, pp. 14-16, Jan. 1999.

[8] P. W. Wolniansky, G. J. Foschini, G. D. Golden, and R. A. Valenzuela, "V-BLAST: an architecture for realizing very high data rates over the rich-scattering wireless channel," *Proc. IEEE International Symposium on Signals, Systems, and Electronics (ISSSE'98)*, Pisa, Italy, Sep.-Oct. 1998, pp. 295-300.

[9] A. Benjebbour, H. Murata, and S. Yoshida, "Comparison of ordered successive receivers for space-time transmission," in *Proc. IEEE 54th Vehicular Technology Conference (VTC'01 Fall)*, Atlantic City, NJ, Oct. 2001, pp. 2053-2057.

[10] S. Alamouti, "A simple transmit diversity technique for wireless comminications," *IEEE J. Sel. Areas Commun.*, vol. 16, no. 8, pp. 1451-1458, Oct. 1998.

[11] V. Tarokh, H. Jafarkhani, and A. R. Calderbank, "Space-time block codes from orthogonal designs," *IEEE Trans. Inform. Theory*, vol. 45, no. 5, pp. 1456-1467, Jul. 1999.

[12] V. Tarokh, N. Seshadri, and A. R. Calderbank, "Space-time codes for high data rate wireless communication: Performance criterion and code construction," *IEEE Trans. Inform. Theory*, vol. 44, no. 2, pp. 744-765, Mar. 1998.

[13] G. L. Stüber, J. R. Barry, S. W. Mclaughlin, Y. Li, M. A. Ingram, and Thomas and G. Pratt, "Broadband MIMO-OFDM wireless communications," *Proc. IEEE*, vol. 92, no. 2, pp. 271-294, Feb. 2004.

[14] G. B. Giannakis, Z. Liu, X. Ma, and S. Zhou, *Space-Time Coding for Broadband Wireless Communications*, Hoboken, NJ, Wiley-Interscience, 2003.

[15] D. Vuletic, W. Lowdermilk, and f. harris, "Advantage and implementation considerations of shaped OFDM signals," in *Proc. 37th Asilomar Conference on Signals, Systems and Computers*, Pacific Grove, CA, Nov. 2003, pp. 683-687.

[16] I. Trigui, M. Siala, S. Affes, A. Stéphenne, and H. Boujemâa, "Optimum pulse shaping for OFDM/BFDM systems operating in time varying multi-path channels," in *Proc. IEEE Globecom'07*, Washington, DC, Nov. 2007, pp. 3817-3821.

[17] H. Bölcskei, "Efficient design of pulse shaping filters for OFDM systems," in *Proc. SPIE on Wavelet Applications in Signal and Image Processing VII*, Denver, CO, USA, Jul. 1999, pp. 625-636.

[18] J. Armstrong, "Analysis of new and existing methods of reducing intercarrier interference due to carrier frequency offset in OFDM," *IEEE Trans. Commun.*, vol. 47, pp. 365-369, Mar. 1999.

[19] N. C. Beaulieu, C. C. Tan, and M. O. Damen, "A 'better than' Nyquist pulse," *IEEE Commun. Lett.*, vol. 5, vol. 9, pp. 367-368, Sep. 2001.

[20] P. Tan and N. C. Beaulieu, "Reduced ICI in OFDM systems using the "better than" raised-cosine pulse," *IEEE Commun. Lett.*, vol. 8, vol. 3, pp. 135-137, Mar. 2004.

[21] H-A M. Mourad, "Reducing ICI in OFDM Systems using a proposed pulse shape," *Wireless Person. Commun.*, vol. 40, pp. 41-48, 2006.

[22] A. Assalini and A. M. Tonello, "Improved Nyquist pulses," *IEEE Commun. Lett.*, vol. 8, vol. 2, pp. 87-89, Feb. 2004.

[23] N. D. Alexandru and A. L. Onofrei, "ICI reduction in OFDM systems using phase modified sinc pulse," *Wireless Person. Commun.*, vol. 53, pp. 141-151, 2010.

[24] P. Tan and N. C. Beaulieu, "Analysis of the effects of Nyquist pulse-shaping on the performance of OFDM systems with carrier frequency offset," *European Transactions on Telecommunications*, vol. 20, pp. 9-22, 2009.

[25] L. E. Franks, "Further results on Nyquist's problem in pulse transmission," *IEEE Transactions Communications Technology*, vol. 16, no. 4, pp. 337-340, 1968.

[26] f. harris, C. Dick, S. Seshagiri, and K. Moerder, "An improved square-root Nyquist shaping filter," in *Proc. Software Defined Radio Technical Conference and Product Exposition*, Orange County, CA, Nov. 2005.

[27] T. Pollet, M. V. Bladel, and M. Moeneclaey, "BER sensitivity of OFDM systems to carrier frequency offset and Wiener phase noise," *IEEE Trans. Commun.*, vol. 43, no. 2/3/4, pp. 191-193, Feb./Mar./Apr. 1995.

[28] H. Nikookar and B. G. Negash, "Frequency offset sensitivity reduction of multicarrier transmission waveshaping," in *Proc. IEEE Conference on Personal Wireless Communications*, Hyderabad, India, Dec. 2000, pp. 444-448.

[29] J. Proakis and M. Salehi, *Digital Communications*, New York, McGraw-Hill, 2007.

[30] W. Weibull, "A statistical distribution function of wide applicability," *J. Appl. Mech.-Trans. ASME*, vol. 18, no. 3, pp. 293-297, 1951.

[31] W. C. Jakes, *Microwave Mobile Communications*, New York, John Wiley & Sons, 1976.

[32] P. Dent, G. E. Bottomley, and T. Croft, "Jakes fading model revisited," *Electron. Lett.*, vol. 29, vol. 13, pp. 1162-1163, Jun. 1993.

[33] K. E. Baddour and N. C. Beaulieu, "Autoregressive modeling for fading channel simulation," *IEEE Wireless Commun.*, vol. 4, no. 4, pp. 1650-1662, Jul. 2005.

[34] IEEE 802.16.3c-01/29r4, "Channel models for fixed wireless applications," *IEEE 802.16 Broadband Wireless Access Working Group*, Jul. 2001.

[35] W. Tranter, K. Shanmugan T. Rappaport, and K. Kosbar, *Communications Systems Simulation with Wireless Applications*, Upper Saddle River, NJ, Prentice Hall, 2004.

[36] M. Debbah and R. Müller, "MIMO channel modeling and the principle of maximim entropy," *IEEE Inf. Theory*, vol. 51, no. 5, pp. 1667-1690, May 2005.

[37] P. Tan and N. C. Beaulieu, "Improved BER performance in OFDM systems with frequency offset by novel pulse-shaping," in *Proc. IEEE Globecom'04*, Dallas, TX, Nov.-Dec. 2004, pp. 230-236.